

**This is a self-archived version of an original article. This version may differ from the original in pagination and typographic details.**

**Author(s):** Zhang, W.; Cederwall, B.; Doncel, M.; Aktas, Ö.; Ertoprak, A.; Qi, C.; Grahn, T.; Nara Singh, B. S.; Cullen, D. M.; Hodge, D.; Giles, M.; Stolze, S.; Auranen, K.; Badran, H.; Braunroth, T.; Calverley, T.; Cox, D. M.; Fang, Y. D.; Greenlees, P. T.; Hilton, J.; Ideguchi, E.; Julin, R.; Juutinen, S.; Kumar Raju, M.; Leino, M.; Li, H.; Liu, H.; Matta, S.; Subramaniam, P.; Modamio, V.; Pakarinen, J.; Papadakis, P.;

**Title:** Decay spectroscopy of  $^{171,172}\text{Os}$  and  $^{171,172,174}\text{Ir}$

**Year:** 2023

**Version:** Published version

**Copyright:** © Authors 2023

**Rights:** CC BY 4.0

**Rights url:** <https://creativecommons.org/licenses/by/4.0/>

**Please cite the original version:**

Zhang, W., Cederwall, B., Doncel, M., Aktas, Ö., Ertoprak, A., Qi, C., Grahn, T., Nara Singh, B. S., Cullen, D. M., Hodge, D., Giles, M., Stolze, S., Auranen, K., Badran, H., Braunroth, T., Calverley, T., Cox, D. M., Fang, Y. D., Greenlees, P. T., . . . Valiente-Dobón, J.J. (2023). Decay spectroscopy of  $^{171,172}\text{Os}$  and  $^{171,172,174}\text{Ir}$ . *Physical Review C*, 107(1), Article 014308.  
<https://doi.org/10.1103/PhysRevC.107.014308>

Decay spectroscopy of  $^{171,172}\text{Os}$  and  $^{171,172,174}\text{Ir}$ 

W. Zhang<sup>1</sup>, B. Cederwall<sup>1</sup>, M. Doncel<sup>2</sup>, Ö. Aktas<sup>1</sup>, A. Ertoprak<sup>1</sup>, C. Qi<sup>1</sup>, T. Grahn<sup>3</sup>, B. S. Nara Singh<sup>4</sup>, D. M. Cullen<sup>5</sup>, D. Hodge<sup>5</sup>, M. Giles<sup>5</sup>, S. Stolze<sup>3</sup>, K. Auranen<sup>3</sup>, H. Badran<sup>3</sup>, T. Braunroth<sup>6</sup>, T. Calverley<sup>3</sup>, D. M. Cox<sup>7</sup>, Y. D. Fang<sup>8,9</sup>, P. T. Greenlees<sup>3</sup>, J. Hilton<sup>3</sup>, E. Ideguchi<sup>8</sup>, R. Julin<sup>3</sup>, S. Juutinen<sup>3</sup>, M. Kumar Raju<sup>8,10</sup>, M. Leino<sup>3</sup>, H. Li<sup>1</sup>, H. Liu<sup>1</sup>, S. Matta<sup>1</sup>, P. Subramaniam<sup>1</sup>, V. Modamio<sup>11</sup>, J. Pakarinen<sup>3</sup>, P. Papadakis<sup>12</sup>, J. Partanen<sup>3</sup>, C. M. Petrache<sup>13</sup>, P. Rahkila<sup>3</sup>, P. Ruotsalainen<sup>3</sup>, M. Sandzelius<sup>3</sup>, J. Sarén<sup>3</sup>, C. Scholey<sup>3</sup>, J. Sorri<sup>3</sup>, M. J. Taylor<sup>3</sup>, J. Uusitalo<sup>3</sup>, and J. J. Valiente-Dobón<sup>14</sup>

<sup>1</sup>*KTH Royal Institute of Technology, 10691 Stockholm, Sweden*

<sup>2</sup>*Department of Physics, Stockholm University, SE-10691 Stockholm, Sweden*

<sup>3</sup>*Accelerator Laboratory, Department of Physics, University of Jyväskylä, FI-40014 Jyväskylä, Finland*

<sup>4</sup>*School of Computing Engineering and Physical Sciences, University of the West of Scotland, Paisley PA1 2BE, United Kingdom*

<sup>5</sup>*Department of Physics and Astronomy, Schuster Building, The University of Manchester, Manchester M13 9PL, United Kingdom*

<sup>6</sup>*Institut für Kernphysik, Universität zu Köln, 50937 Köln, Germany*

<sup>7</sup>*Department of Physics, Lund University, 221 00 Lund, Sweden*

<sup>8</sup>*Research Center for Nuclear Physics, Osaka University, JP-567-0047 Osaka, Japan*

<sup>9</sup>*Institute of Modern Physics, Chinese Academy of Sciences, Lanzhou 730000, China*

<sup>10</sup>*Department of Physics, GITAM Institute of Science, GITAM University, Visakhapatnam 530045, India*

<sup>11</sup>*Department of Physics, University of Oslo, NO-0316 Oslo, Norway*

<sup>12</sup>*STFC Daresbury Laboratory, Daresbury, Warrington WA4 4AD, United Kingdom*

<sup>13</sup>*Université Paris-Saclay, CNRS/IN2P3, IJCLab, 91405 Orsay, France*

<sup>14</sup>*Istituto Nazionale di Fisica Nucleare, Laboratori Nazionali di Legnaro, I-35020 Legnaro, Italy*



(Received 13 October 2022; accepted 11 January 2023; published 19 January 2023)

We report on a study of the  $\alpha$ -decay fine structure and the associated  $E_\alpha$ - $E_\gamma$  correlations in the decays of  $^{171,172}\text{Os}$  and  $^{171,172,174}\text{Ir}$ . In total, 13 new  $\alpha$ -decay energy lines have been resolved, and three new  $\gamma$ -ray transitions have been observed following the new decay branches to  $^{168}\text{Re}$  and  $^{167}\text{W}$ . The weak  $\alpha$ -decay branch from the bandhead of the  $\nu i_{13/2}$  band in  $^{171}\text{Os}$  observed in this work highlights an unusual competition between  $\alpha$ ,  $\beta$ , and electromagnetic decays from this isomeric state. The nucleus  $^{171}\text{Os}$  is therefore one of few nuclei observed to exhibit three different decay modes from the same excited state. The nuclei of interest were produced in  $^{92}\text{Mo}(^{83}\text{Kr}, x\text{pyn})$  fusion-evaporation reactions at the Accelerator Laboratory of the University of Jyväskylä, Finland. The fusion products were selected using the gas-filled ion separator RITU and their decays were characterized using an array of detectors for charged particles and electromagnetic radiation known as GREAT. Prompt  $\gamma$ -ray transitions were detected and correlated with the decays using the JUROGAM II germanium detector array surrounding the target position. Results obtained from total Routhian surface (TRS) calculations suggest that  $\alpha$ -decay fine structure and the associated hindrance factors may be a sensitive probe of even relatively small shape changes between the final states in the daughter nucleus.

DOI: [10.1103/PhysRevC.107.014308](https://doi.org/10.1103/PhysRevC.107.014308)

## I. INTRODUCTION

Neutron-deficient nuclides in the transitional tungsten-rhenium-osmium-iridium-platinum region exhibit interesting nuclear phenomena such as shape coexistence [1] and the recently discovered anomalous  $B(E2)$  values at low excitation energies [2–6]. The ground states in these nuclei are char-

acterized by a competition between  $\alpha$ ,  $\beta$ , and, for the most neutron deficient species, also proton emission. Additionally, this applies to some long-lived isomeric states for which heavy charged particle emission and  $\beta$  decay may compete with the internal electromagnetic transitions. Shape changes may favorably be probed by  $\alpha$ -decay properties since the hindrance degree of this decay process provides information on the change in nuclear structure between the connected states, in particular the associated shapes [7]. Nuclei in this region of the nuclear chart are predicted to be characterized by varying and moderately deformed shapes [8]. Their low-lying excited states are dominated by configurations with the valence neutrons occupying levels emanating from the  $\nu f_{7/2}$ ,  $\nu h_{9/2}$ , or  $\nu i_{13/2}$  spherical subshells while the proton Fermi level is situated close to single-particle levels dominated by

Published by the American Physical Society under the terms of the [Creative Commons Attribution 4.0 International](https://creativecommons.org/licenses/by/4.0/) license. Further distribution of this work must maintain attribution to the author(s) and the published article's title, journal citation, and DOI. Funded by [Bibsam](https://www.bibsam.com/).

configurations with the  $\pi s_{1/2}$ ,  $\pi d_{3/2}$ , and  $\pi h_{11/2}$  parentage. Large changes in angular momentum are required for internal transitions between the states in odd- $Z$  nuclei where the odd proton populates an orbital dominated by the  $\pi h_{11/2}$  parentage and those built on  $\pi s_{1/2}$  or  $\pi d_{3/2}$  configurations. This generally leads to a corresponding high-spin or low-spin  $\alpha$ -decaying state, respectively, in odd- $Z$ , even- $N$  or in odd-odd nuclei in the region. This paper reports on a study of the fine structure in the  $\alpha$  decay of  $^{171,172}\text{Os}$  and  $^{171,172,174}\text{Ir}$ .

## II. EXPERIMENTAL DETAILS

The experiment was performed at the Accelerator Laboratory of the University of Jyväskylä (JYFL), Finland. A  $^{83}\text{Kr}$  beam was accelerated to 383 MeV by the K130 cyclotron and used to bombard a  $0.52 \text{ mg cm}^{-2}$  thick, isotopically enriched,  $^{92}\text{Mo}$  target foil with an average beam intensity of  $\approx 2$  particle nA during 12 days. This experiment was primarily aimed at measuring lifetimes of excited states [4,5] using a differential plunger device for unbound nuclear states [9]. Prompt  $\gamma$  rays emitted at the target position were measured by the JUROGAM II germanium detector array (JGII), which comprised 15 Eurogam Phase I-type [10] and 24 Euroball clover [11] Compton-suppressed high-purity germanium (HPGe) detectors. Fusion-evaporation reaction products were transported by the gas-filled ion separator RITU [12] to its focal plane detector system, the GREAT spectrometer [13]. At the focal plane, recoils were passed through a multiwire proportional counter before being implanted into two adjacently mounted double-sided silicon strip detectors (DSSDs). Each DSSD was  $300 \mu\text{m}$  thick, with an active area of  $60 \text{ mm} \times 40 \text{ mm}$ , and the strip pitch was 1 mm wide on both faces, thus yielding 4800 independent pixels. Located downstream of the DSSDs was a double-sided planar HPGe detector [13,14], which was used to measure  $\gamma$  rays and x rays emitted during decay processes in the DSSDs. The data streaming from the JGII and the GREAT spectrometers were recorded and merged using the triggerless Total Data Readout (TDR) data acquisition system with a global 100 MHz clock [15,16].

## III. DATA ANALYSIS AND RESULTS

In total,  $\approx 3.6 \times 10^8$  evaporation residues were implanted into the DSSDs at an average rate of 350 Hz, with the most abundant reaction products being  $^{172}\text{Os}$  and  $^{171}\text{Os}$ . Figure 1 shows the total  $\alpha$ -decay energy spectrum obtained in the experiment with a relatively long time window of 60 s applied to the recoil- $\alpha$  correlations in order to study long-lived nuclei such as  $^{172}\text{Os}$  which has a known half-life of 19.2(9) s [17]. In such cases, special care has to be taken as the implantation rate limits the use of the RDT technique [18] to correlate  $\alpha$  decays with the true mother recoil. However, the recoil implantation was not uniformly distributed in the DSSDs, as shown in Fig. 2, showing the detected  $\alpha$  distribution across the horizontal strips of the DSSDs. Since the count rate in the tail strips was more than an order of magnitude lower than that of the central strips, it was possible to largely eliminate random correlations in the study of long-lived nuclei by selecting

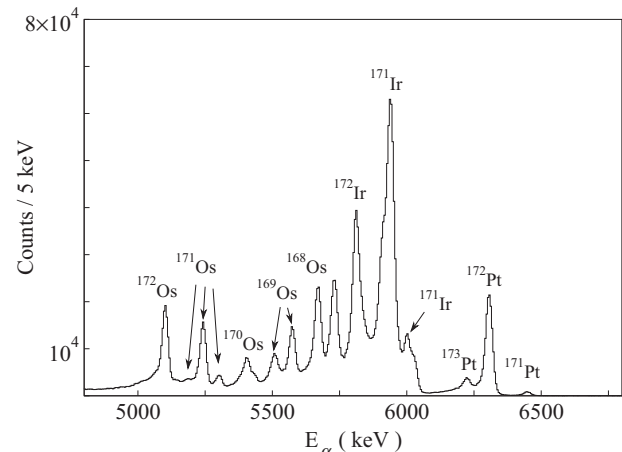


FIG. 1. Total  $\alpha$ -particle energy spectrum observed in the DSSDs. Assignments to the main  $\alpha$  decay lines are indicated.

events in these peripheral strips. The energy calibration of the DSSDs was accomplished using a mixed-element radioactive source ( $^{244}\text{Cm}$ ,  $^{241}\text{Am}$ , and  $^{239}\text{Pu}$ ) with its three dominant  $\alpha$  energy lines. On account of the well known pulse height defect for heavy ions [19] and the dead layer at the front face of the DSSD which is typically approximately  $1 \mu\text{m}$  or less [20], the measured  $\alpha$ -decay energy using such a calibration differs slightly from the total energy released during the decay process. This effect was corrected using the known  $\alpha$ -particle kinetic energies ( $E_\alpha$ ) of  $^{168}\text{Os}$ ,  $^{171}\text{Pt}$ , and  $^{172}\text{Pt}$  [17,21] nuclides produced in the experiment. The energy calibration of the planar HPGe detector was done using the standard radioactive  $\gamma$ -ray sources  $^{133}\text{Ba}$  and  $^{152}\text{Eu}$ , and the efficiency calibration was taken from Monte Carlo simulations [14].

### A. $\alpha$ decay of $^{172}\text{Os}$

The energy of the  $\alpha$  particles ( $E_\alpha$ ) from the  $\alpha$  decay of the ground state of  $^{172}\text{Os}$  to the ground state of  $^{168}\text{W}$ , as can be seen in Fig. 1, was measured from the present experiment to be 5106(4) keV, which is in a good agreement with the previous measurements [17]. To extract its corresponding lifetime,

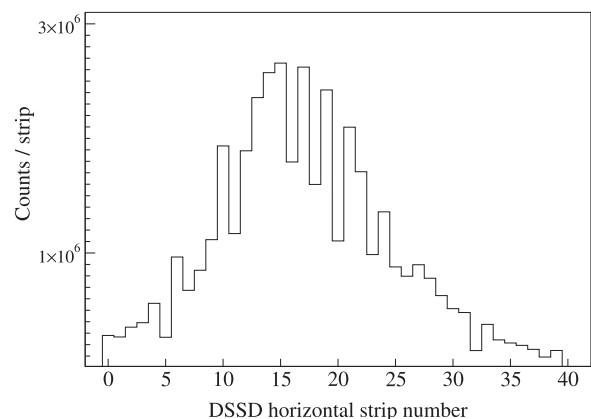


FIG. 2. The distribution of detected  $\alpha$  events in the horizontal strips of the DSSDs accumulated during the entire experiment.

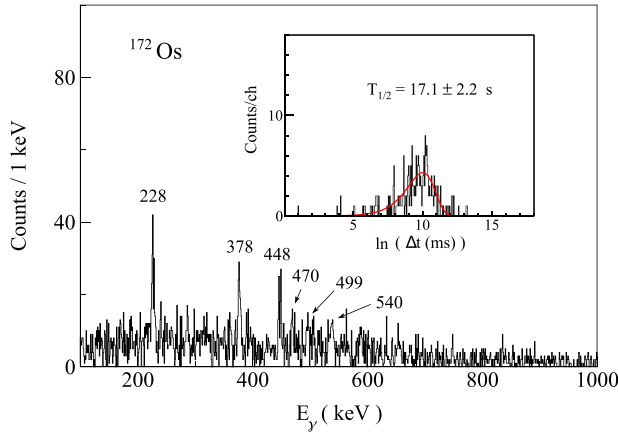


FIG. 3. Prompt RDT  $\gamma$  rays in JGII correlated with recoil implantations in the DSSDs followed by the  $E_\alpha = 5106$  keV  $\alpha$  decay of  $^{172}\text{Os}$  within a maximum search time of 1 minute in the same pixel. The inset shows the time difference spectrum of the correlated recoil- $\alpha$  events within a search time of 10 minutes by gating on the prompt 228 keV  $\gamma$  rays. The fit to the logarithmic time distribution was produced using the Schmidt formula [22] indicated by the red line.

the low-counting horizontal DSSD strips with the strip number larger than 33 (Fig. 2) were used for the search of recoil- $\alpha$  correlations. Figure 3 shows the energies of prompt  $\gamma$  rays detected in JGII in delayed coincidence with this  $\alpha$  decay under this condition, demonstrating that a clean selection of  $\alpha$  recoil can be obtained in this way. As shown in the inset of Fig. 3, the time distribution of the  $E_\alpha = 5106$  keV decay was obtained by tagging on the prompt 228 keV  $\gamma$  rays of  $^{172}\text{Os}$ , and its half-life was determined to be 17.1(2.2) s, consistent with the previously reported values [23,24]. The determination of the branching ratio of this  $\alpha$  decay was performed by measuring the ratio of the intensity of the prompt 228 keV  $2_1^+ \rightarrow 0_{gs}^+$   $\gamma$ -ray transition in  $^{172}\text{Os}$  detected by JGII for recoil-tagged and recoil- $\alpha$ -tagged events. To suppress the contamination from other reaction channels, we applied prompt  $\gamma$ - $\gamma$  coincidence cuts by gating on the higher-lying 378, 448, or 470 keV transitions in the yrast cascade of  $^{172}\text{Os}$  in JGII. Assuming a detection efficiency of 55(5)% for full  $\alpha$  energy measured in the DSSDs, a branching ratio  $b_\alpha = 1.2(3)\%$  was obtained for this  $\alpha$  decay, which agrees well with the previously measured value of  $b_\alpha = 1.1(2)\%$  [24].

Figure 4 depicts a two-dimensional  $E_\alpha$ - $E_\gamma$  spectrum with a condition of  $0 < \Delta t(\gamma-\alpha) < 300$  ns, where the  $\gamma$  rays were detected by the planar HPGe detector at the focal plane and the  $\alpha$  decays were measured using all DSSD strips. A few known groups of  $\alpha$ - $\gamma$  events and new weak  $\alpha$ -decay branches identified in the present work for  $^{171,172}\text{Os}$  are marked with their corresponding energies. The long ridges passing through the 92.1 and 162.1 keV  $\gamma$ -ray energies are due to the tails of the peaks of the 5919 and 5818 keV  $\alpha$  particles from the decay of  $^{171}\text{Ir}$  and  $^{172}\text{Ir}$ , respectively. Such tails results from incomplete charge collection and  $\alpha$  particles escaping the DSSDs. The group at  $E_\alpha(4909$  keV)- $E_\gamma(199.2$  keV) represents the identification of a new  $\alpha$  decay which we assign as the ground-

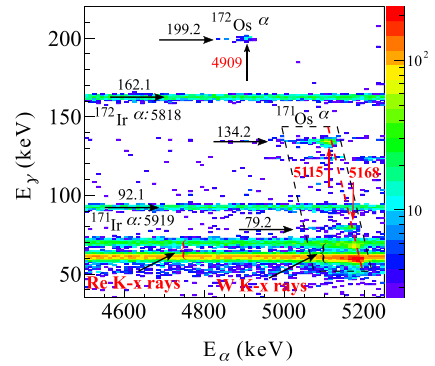


FIG. 4.  $E_\alpha$ - $E_\gamma$  coincidence spectrum selected from events with the correlation time interval of  $< \Delta t(\gamma-\alpha) < 300$  ns. All energies are given in keV. Each group is indicated with the corresponding energies and the arrows indicate the positions of the associated  $\alpha$  particles and  $\gamma$  rays; see details in the text.

state decay of  $^{172}\text{Os}$  to the first  $2^+$  excited state of  $^{168}\text{W}$ . The assignment is based on the total Q value,  $Q_{\alpha,\text{tot}} = 5225(5)$  keV extracted from  $E_\alpha = 4909(5)$  keV and  $E_\gamma = 199.2$  keV, which agrees well with  $Q_{\alpha,\text{tot}} = 5228(4)$  keV calculated from  $E_\alpha = 5106(4)$  keV for the ground-state to ground-state  $\alpha$  decay. A ratio of 0.0059(12)% was deduced for the new  $\alpha$  branch with an efficiency  $\epsilon(199.2) = 0.092(8)$  of the planar detector at 199.2 keV, taken from simulations [14]. For the following discussion, it is noteworthy that all  $\gamma$ -ray and x-ray intensities measured with the planar HPGe detector were corrected for the respective efficiencies as derived from Monte Carlo simulations [14] when deriving internal conversion coefficients and branching ratios as described below. Using the  $\alpha$  events associated with the delayed 199.2 keV  $\gamma$ -ray transition and detected at the low-counting horizontal DSSD strips (the same as the aforementioned selection for the  $E_\alpha = 5106$  keV decay in the search of recoil- $\alpha$  correlations), a half-life of  $18_{-6}^{+10}$  s was achieved through a maximum likelihood analysis [22], in agreement with the previously determined half-life from the ground-state to ground-state  $\alpha$ -decay of  $^{172}\text{Os}$  [17]. The results for  $^{172}\text{Os}$  obtained from the present work are summarized in Table I and the deduced decay scheme is shown in Fig. 7.

## B. $\alpha$ -decay of $^{171}\text{Os}$

The sloped parallelogram region drawn in Fig. 4 highlights the observed fine structure of the ground-state  $\alpha$  decay of  $^{171}\text{Os}$  including the groups at  $E_\alpha(5168$  keV)- $E_\gamma(79.2$  keV), the new  $\alpha$ - $\gamma$  coincidence pair  $E_\alpha(5115$  keV)- $E_\gamma(134.2$  keV), and  $\alpha$  particles correlated with tungsten K x rays. The  $E_\alpha = 5168$  keV decay was reported previously in Ref. [24] and an  $M1$  multipolarity was assigned to the subsequent 79.2 keV  $\gamma$ -ray transition. The  $K$ -shell internal-conversion coefficient of the 79.2 keV transition was deduced to be 9.0(11) in this work, consistent with the theoretical value of 7.8(2) for the  $M1$  multipolarity [25]. Careful scrutiny of Fig. 4 reveals that the  $\alpha$ -particle energies associated with tungsten K x rays are affected by the known effect of  $\alpha$  particle-conversion electron energy summing in the DSSD [26]. A value of the  $K$ -shell

TABLE I. Measured  $\alpha$ -decay energies,  $E_\alpha$  (coincident  $E_\gamma$ , if observed), half-life values  $T_{1/2}$ , branching ratios  $b_\alpha$ , formation probabilities  $|RF_i(R)|^2$ , reduced widths, relative hindrance factors (HF) (when possible) referenced to the  $\alpha$  decay of  $^{170}\text{Os}$  with  $E_\alpha = 5.407$  MeV, tentative spin and parity assignments as proposed from this work or quoted from the earlier studies, and the deduced internal conversion coefficients as well as the multiplicities (when possible) for  $^{171,172}\text{Os}$  and  $^{171,172,174}\text{Ir}$ .

Nucleus	$J_i^\pi$	$T_{1/2}$ (s)	$E_\alpha$ (keV)	$b_\alpha$ (%)	$ RF_i(R) ^2$ (fm $^{-1}$ )	$\delta^2$ (keV)	HF	$J_f^\pi$	$E_\gamma$ (keV)	$\alpha_k$	Multiplicity
$^{170}\text{Os}$ [17]	$0^+$	7.37(18)	5407(2)	9.5(10)	0.012(1)	117(12)	1	$0^+$			
$^{172}\text{Os}$	$0^+$	17.1(2.2)	5106(4)	1.2(3)	0.019(5)	182(51)	0.6(2)	$0^+$			
$^{172}\text{Os}$			4909(5)	0.0059(12)	0.0017(4)	17(4)	7(2)	$2^+$	199.2(3)		$E2$
$^{171}\text{Os}$	$(5/2^-)$ [28]	8.0(4)	5248(4)	1.68(18) [17]	0.011(1)	109(12)	1.1(1)	$(5/2^-)$ [17]			
$^{171}\text{Os}$			5168(4)	0.096(14)	0.0029(4)	28(4)	4.2(7)	$(7/2^-)$ [17]	79.2(3)	9.0(11)	$M1$
$^{171}\text{Os}$			5115(4)	0.037(11)	0.0021(6)	20(6)	6(2)	$(9/2^-)$	134.2(3)	0.39(8)	$E2$
$^{171}\text{Os}$	$(13/2^+)$ [28]	0.79(2)	5306(4)	0.21(5)	0.0076(18)	72(17)	1.6(4)	$(13/2^+)$			
$^{171}\text{Ir}$	$(11/2^-)$ [31]	1.28(4)	5919(4)	53(5) [31]	0.0067(6)	61(6)	1.9(3)	$(11/2^-)$ [31]	92.1(2)	5.1(4)	$M1$
$^{171}\text{Ir}$			6011(5)	9(1) <sup>a</sup>	0.0008(1)	7.8(9)	15(2)	$(9/2^-)$			
$^{172}\text{Ir}$	$(7^+)$ [33]	1.89(5)	5818(4)	9.5(11) [33]	0.0020(2)	19(2)	6.2(9)	$(7^+)$ [33]	162.1(2)	0.69(6)	$M1/E2$ [34]
$^{172}\text{Ir}$			5755(7)	<0.004					224.0(6)		
$^{172}\text{Ir}$	$(3^-, 4^-)$ [33]	4.1(2)	5547(5)	0.36(6) <sup>b</sup>					89.4(3)		$E1^c$
$^{172}\text{Ir}$			5537(5)	0.15(3) <sup>b</sup>					102.8(3)		$E1^c$
$^{172}\text{Ir}$			5517(5)	1.15(20) <sup>b</sup>					123.0(2)		$E1$ [34]
$^{172}\text{Ir}$			5505(5)	0.34(6) <sup>b</sup>					136.0(2)		$E1^c$
$^{174}\text{Ir}$	$(3^+)$ [34]	7.1(22) <sup>d</sup>	5292(8)	0.23(3) <sup>e</sup>					193.1(4)		$E2^f$
$^{174}\text{Ir}$			5268(5)	0.17(2) <sup>e</sup>					224.0(6)		$E2^f$
$^{174}\text{Ir}$	$(7^+)$ [34]	4.4(1.1) <sup>g</sup>	5499(8)	0.4(1) <sup>h</sup>					191(1)		$E1^i$
$^{174}\text{Ir}$			5476(5)	1.8(6) <sup>h</sup>					210.1(3)		$E2^j$

<sup>a</sup>This value was obtained by assuming that the 53(5)% branching ratio reported in Ref. [31] corresponds to the 5919 keV line.

<sup>b</sup>A total branching ratio  $b_\alpha = 2.0(2)\%$  [34] is divided among the four  $\alpha$  decays.

<sup>c</sup>Assumption based on the multipolarity assignment of the 123.0 keV transition in [34].

<sup>d</sup>This was determined by gating on the 193.1 or 224 keV transitions.

<sup>e</sup>A total branching ratio  $b_\alpha = 0.4\%$  [34] is divided between the 5292 and 5268 keV  $\alpha$  decays.

<sup>f</sup>Assumption based on the measurement in [34].

<sup>g</sup>This was determined by gating on the 191 or 210.1 keV transitions.

<sup>h</sup>A total branching ratio  $b_\alpha = 2.2(3)\%$  [34] is divided between the 5476 and 5499 keV  $\alpha$  decays.

<sup>i</sup>Suggested in [34].

<sup>j</sup>Suggested in [34].

internal-conversion coefficient for the 134.2 keV transition which is associated with the new  $E_\alpha = 5115$  keV decay branch is determined to be 0.39(8), in good agreement with the theoretical value of 0.47 for an  $E2$  multipolarity [25]. The total deduced  $Q_{\alpha,\text{tot}}$  value agrees well with that of the other observed decay branches within the experimental uncertainties, i.e.,  $Q_{\alpha,\text{tot}} = 5372(5)$  keV for the  $E_\alpha = 5115(4)$  keV decay, 5371(4) keV for the  $E_\alpha = 5168(4)$  keV decay, and 5374(4) keV for the  $E_\alpha = 5248(4)$  keV decay. Based on these arguments as well as on the obtained half-life as shown below, we tentatively assign the new 5115(4) keV  $\alpha$  particles to be emitted in the decay of the  $(5/2^-)$  ground state of  $^{171}\text{Os}$  to a  $(9/2^-)$  excited state of  $^{167}\text{W}$ . Its branching ratio was determined to be 0.037(11)% by comparing its intensity to that of the  $E_\alpha = 5248$  keV decay with the known branching ratio 1.68(18)% [17]. Similarly, the branching ratio of the  $E_\alpha = 5168$  keV decay was determined to be 0.096(14)%, in agreement with the adopted value 0.117(14)% in the NNDC database [17]. To extract the half-lives of these  $\alpha$  decays, we chose a relatively larger DSSD area compared to the case of  $^{172}\text{Os}$ , with the strip number of the horizontal DSSD strips

larger than 28 or smaller than 6. The obtained half-lives are 8.0(4), 8.5(12), and 8.2(14) s for the  $E_\alpha = 5248(4)$ , 5168(4), and 5115(4) keV decays of the ground-state of  $^{171}\text{Os}$ , respectively, and the weighted average half-life value for this state is 8.0(4) s in good agreement with the adopted value  $T_{1/2} = 8.3(2)$  s [17].

A second new  $\alpha$  decay of  $^{171}\text{Os}$  was observed with  $E_\alpha = 5306(4)$  keV, as indicated in Fig. 1. Although  $\alpha$  particles at the same energy were seen in the spectrum of Fig. 5.1 of Ref. [27], they were not assigned to any nucleus. Here, with the help of the prompt RDT  $\gamma$  rays of  $^{171}\text{Os}$  in JGII as shown in Fig. 5, we could firmly assign this decay to  $^{171}\text{Os}$ . It is also clearly shown in Fig. 5 that there are no significant  $\gamma$ -ray transitions other than those belonging to the known  $i_{13/2}$  band of  $^{171}\text{Os}$  [28] present in the RDT-gated spectrum. Therefore, we assign these 5306(4) keV  $\alpha$  particles to be emitted in the decay of the bandhead  $(13/2^+)$  state of the  $\nu i_{13/2}$  band in  $^{171}\text{Os}$  to the bandhead  $(13/2^+)$  state of  $^{167}\text{W}$ . Moreover, its half-life is determined to be 790(16) ms which is much shorter than the half-life of the  $\alpha$  decay of the  $(5/2^-)$  ground-state. Following the  $\alpha$ -decay energies of  $^{171}\text{Os}$ , the  $(13/2^+)$  state

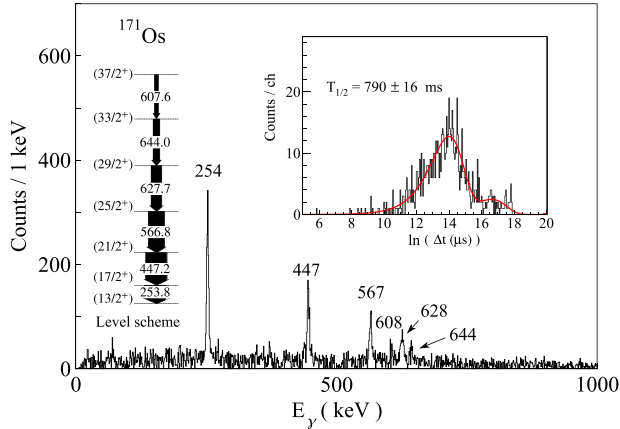


FIG. 5. Prompt RDT  $\gamma$  rays in JGII associated with the  $^{171}\text{Os}$  ion implantation in the DSSDs followed by the  $\alpha$  decay of  $E_\alpha = 5306$  keV within a maximum search time of 10 s in the same pixel. The inset shows the logarithmic time spectrum of the correlated recoil- $\alpha$  events within a search time of 1 minute by gating on prompt 254 keV  $\gamma$  rays. The time distribution was fitted using a two-component Schmidt formula [22] as shown by the red line, and the component at higher  $\ln(\Delta t)$  values corresponds to the random-correlated events. A partial level scheme of the  $\nu i_{13/2}$  band in  $^{171}\text{Os}$  reproduced from the NNDC database [17] is shown in the inset.

of  $^{167}\text{W}$  would lie at an excitation energy of 127(4) keV above the  $(5/2^-)$  state. This confirms the previously tentative assignment of the position of the  $(13/2^+)$  state proposed in Refs. [17,24], in which the bandhead  $(13/2^+)$  state is located above the  $(5/2^-)$  state at an energy of 126 keV based on the assumption that the 79.2 keV  $\gamma$ -ray transition could be described as built on the  $(5/2^-)$   $\alpha$ -decaying bandhead, even though there was previously no direct evidence demonstrating the 79.2 keV  $\gamma$ -ray transition to be in coincidence with the  $\gamma$ -ray transitions in the cascade within the  $(5/2^-)$  band.

The branching ratio for this new  $\alpha$  decay was obtained by measuring the ratio of the recoil-tagged to the recoil- $\alpha$ -tagged intensities of the 254 keV  $\gamma$ -ray transition in coincidence with the prompt 447, 567, or 628 keV  $\gamma$ -ray transitions. An energy spectrum of  $\alpha$  particles in correlation with these recoil- $\gamma$ - $\gamma$  events is shown in Fig. 6, in which the ratio of the events in the 5306 and 5248 keV  $\alpha$ -particle peaks is 0.35(9). Considering the branching ratio 1.68(18)% of the  $E_\alpha = 5248$  keV decay from the  $(5/2^-)$  ground state [17] as well as the detection efficiency of 55(5)% for these  $\alpha$  particles, the branching ratio of the  $E_\alpha = 5306$  keV decay from the  $(13/2^+)$  isomeric state is deduced to be 0.21(5)% and the branching ratio of the isomeric transitions (IT) from the  $(13/2^+)$  state to the  $(5/2^-)$  ground-state is 36(6)%, which means this isomeric state also has a  $\approx 64(6)\%$  possibility to deexcite either by  $\beta^+$  decay or electron capture to  $^{171}\text{Re}$ . Since there were no  $\gamma$ -ray transitions observed in the internal decay from the  $(13/2^+)$  isomeric state to the  $(5/2^-)$  ground state of  $^{171}\text{Os}$ , it is assumed that the decay path might proceed via one or several highly converted transitions. Assuming a single  $\gamma$ -ray transition Weisskopf estimates for multipolarities of  $M3$  or  $E3$  would give the respective partial half-lives of 8.5 and 0.13 s.

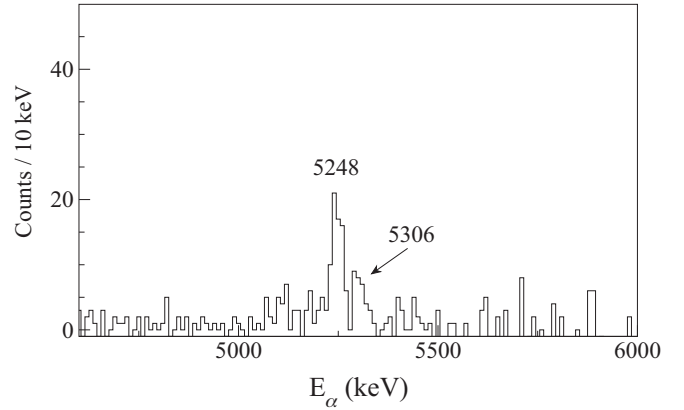


FIG. 6. Energy spectrum of  $\alpha$  decays in correlation with  $^{171}\text{Os}$  recoil implantations and requiring additionally prompt  $\gamma$ - $\gamma$  coincidences between the 254 keV  $\gamma$ -ray transition and either the 447, 567, or 628 keV  $\gamma$ -ray transitions of the  $\nu i_{13/2}$  band. Only the low-counting horizontal DSSD strips with the strip number larger than 28 or smaller than 6 were used for the analysis.

In the neighboring nucleus  $^{169}\text{Os}$ , a similar  $(13/2^+)$  state has been assigned to decay via a tentative and unobserved 80 keV  $M2$  transition to an intermediate 112 keV excited  $(9/2^-)$  state [29]. The  $(13/2^+)$  state in  $^{169}\text{Os}$  was determined to have a half-life of  $T_{1/2} = 17.3(12)$   $\mu\text{s}$ . If the electromagnetic decay of the  $(13/2^+)$  state in  $^{171}\text{Os}$  proceeds in a similar fashion, an  $M2$  transition depopulating this state would have a considerably lower energy and/or the transition would be subject to additional hindrance due to structural differences between the initial and final states. The observed competition between  $\alpha$ ,  $\beta$ , and electromagnetic decays from the same state is unusual and may be used to constrain theoretical models. The results derived from this work related to the  $\alpha$  decay of  $^{171}\text{Os}$  are listed in Table I and also shown in the proposed decay scheme in Fig. 7.

### C. $\alpha$ -decay fine structure of $^{171}\text{Ir}$

The  $\alpha$  decay of  $^{171}\text{Ir}$  has been investigated in several measurements [21,27,30–32] and the decay of the high-spin isomeric  $(11/2^-)$  state is known to be followed by a 92 keV  $M1$   $\gamma$ -ray transition in  $^{167}\text{Re}$ . In these measurements, the half-life values agree well within the experimental uncertainties, with a weighted value of 1.4(1) s [17]. However, the measured energy value  $E_\alpha$  varies considerably from 5920(4) to 5950(5) keV. In the present work, the value  $E_\alpha = 5919(4)$  keV was obtained by combining two different methods; one by tagging on prompt  $\gamma$  rays of  $^{171}\text{Ir}$  detected by JGII and the other one by tagging on the delayed 92 keV  $\gamma$  rays detected by the planar HPGe detector at the focal plane. As shown in Fig. 8, the measured  $E_\alpha$  energies are found to be offset from each other by about 30 keV which represents the energy of  $K$ -conversion electrons of the 92 keV  $M1$  transition. It is then readily concluded that the higher energy value obtained in the previous measurements for this  $\alpha$ -decay is because of the  $\alpha$ - $e^-$  summing effect in the DSSD resulting from the large  $K$ -shell conversion of the 92 keV  $\gamma$ -ray transition. The

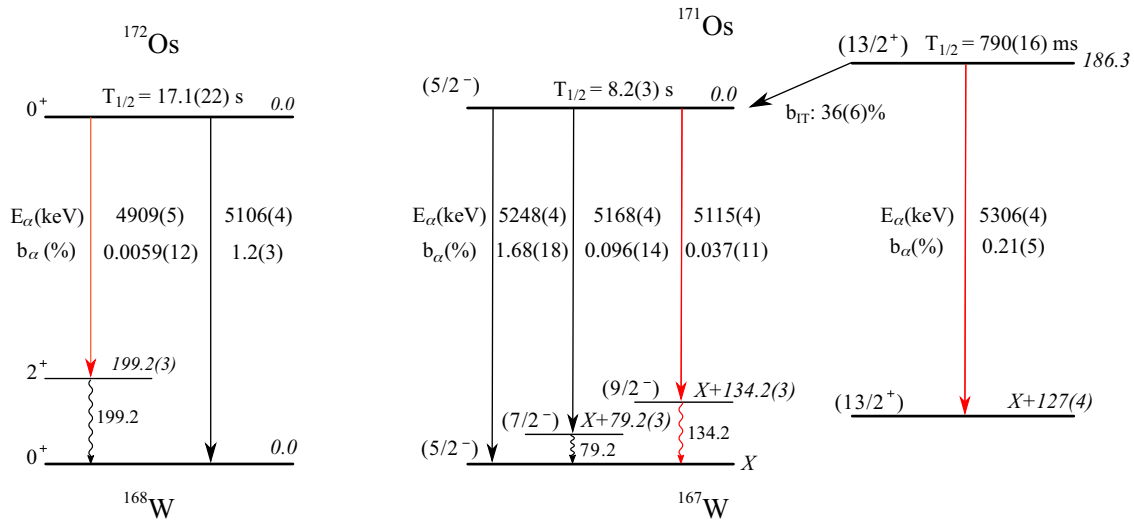


FIG. 7. Decay schemes of  $^{172}\text{Os}$  and  $^{171}\text{Os}$  deduced in this work apart from the branching ratio 1.68(18)% for the 5248 keV  $\alpha$  decay, taken from Ref. [17]. The energy of the  $(5/2^-)$   $\alpha$ -decaying bandhead of  $^{167}\text{W}$  is not established experimentally, and thus is tentatively indicated by X. The newly observed transitions are indicated in red. The determined half-life for each state from this work is shown above the state. See text and Table I for details.

K-shell conversion coefficient that we derived is 5.1(4) which is consistent with the theoretical value of 5.4 for an  $M1$  multipolarity [25].

In addition, a new  $\alpha$ -decay branch was observed for  $^{171}\text{Ir}$  with  $E_\alpha = 6011(5)$  keV, as indicated in the prompt JGII- $\gamma$  tagged spectrum (blue) of Fig. 8. The total  $Q_{\alpha,\text{tot}} = Q_\alpha + E_\gamma(92.1)$  value for the  $E_\alpha = 5919(4)$  keV decay is 6153(4) keV, which matches well with the  $Q_\alpha$  value 6155(5) keV for the  $E_\alpha = 6011(5)$  keV decay. Following this as well as the previous assignment for the  $E_\alpha = 5919(4)$  keV decay [31], it is readily understood as the  $E_\alpha = 6011(5)$  keV decay from the  $(11/2^-)$  state of  $^{171}\text{Ir}$  to the  $(9/2^-)$  state of  $^{167}\text{Re}$ . Referring

to the previously measured 53(5)% branching ratio of the  $E_\alpha = 5919(4)$  keV decay [31], the branching ratio of the new  $E_\alpha = 6011(5)$  keV decay was determined to be 9(1)%. The measured half-lives from the present work are 1280(45) ms and 1255(70) ms as deduced from the  $E_\alpha = 5919(4)$  keV and  $E_\alpha = 6011(5)$  keV decays, respectively. The weighted average,  $T_{1/2} = 1.28(4)$  s, is given in Fig. 8 and Table I.

#### D. $\alpha$ -decay fine structure of $^{172}\text{Ir}$

The  $\alpha$ -decaying low-spin isomeric state ( $3^-$  or  $4^-$ ) [33] of  $^{172}\text{Ir}$  was previously reported to decay to an excited state of  $^{168}\text{Re}$  through an  $E_\alpha = 5.51(1)$  MeV decay with the branching ratio of  $\approx 2\%$ , followed by three  $\gamma$ -ray transitions with energies 89.4(2), 123.0(1), and 136.0(1) keV feeding the low-spin isomeric state of  $^{168}\text{Re}$  [33,34]. It was found in the present work that these  $\gamma$ -ray transitions each correspond to their own respective  $\alpha$ -decay branch, as established from the  $\alpha$ - $\gamma$  coincidences in the parallelogram region of Fig. 9(a). Another new  $\gamma$ -ray transition of 102.8 keV was also observed in correlation with its corresponding  $\alpha$  decay. The  $\alpha$  decays were detected using all DSSD strips and the  $\gamma$  rays were measured by the planar HPGe detector at the RITU focal plane. The correlation time condition on each  $\alpha$ - $\gamma$  event was  $0 < \Delta t(\gamma-\alpha) < 300$  ns. A few previously known groups of  $\alpha$ - $\gamma$  events are marked in the two-dimensional spectrum with their corresponding  $\gamma$ -ray energies. It includes the groups at the  $\gamma$ -ray energies of 92.1 and 162.1 keV associated with the respective  $^{171,172}\text{Ir}$  isotopes as indicated in Fig. 4, and the group at  $\alpha(5666 \text{ keV})$ - $\gamma(136.1 \text{ keV})$  related to  $^{173}\text{Ir}$  [34], as well as the groups at the  $\gamma$ -ray energies of 43 and 73.6 keV correlated with the  $\alpha$  decays of  $^{169}\text{Os}$  [24].

Figure 9(b) illustrates the energy spectra from the projections of the  $\alpha$ - $\gamma$  matrix to the  $\alpha$ -particle energy axis by gating on the respective  $\alpha$ -delayed  $\gamma$  ray. This analysis allowed us to identify these four groups of coincident  $\alpha$ - $\gamma$

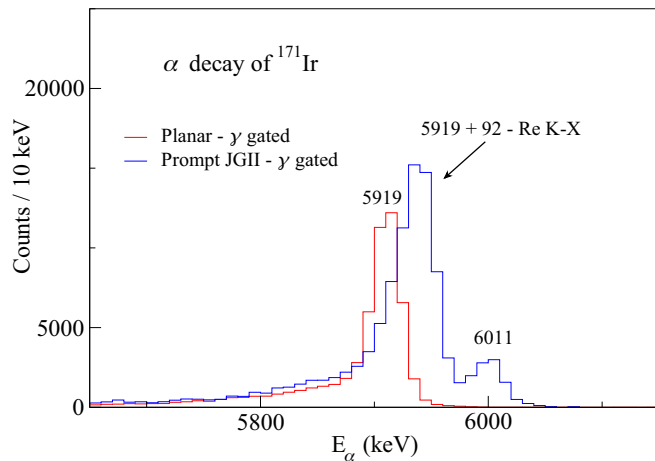


FIG. 8. Energy spectra of alpha particles from the decay of  $(11/2^-)$  state of  $^{171}\text{Ir}$ , the blue one tagged with prompt  $\gamma$  rays from the  $(11/2^-)$  band of  $^{171}\text{Ir}$  and the red one tagged with delayed 92 keV  $\gamma$  rays from  $^{167}\text{Re}$ . Only the low-counting horizontal DSSD strips with the strip number larger than 25 or smaller than 10 were used for the analysis.

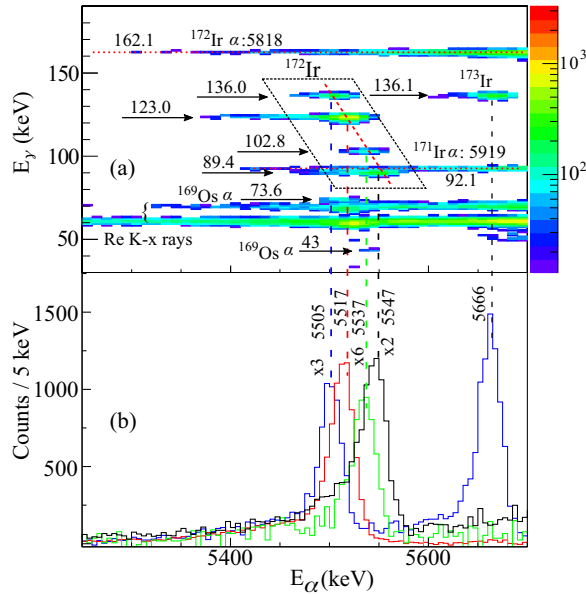


FIG. 9. (a)  $E_\alpha$ - $E_\gamma$  coincidence spectrum with the time interval of  $0 < \Delta t(\gamma-\alpha) < 300$  ns. Each group is indicated with the corresponding energies. The parallelogram region indicates  $\alpha$  decays from the low-spin isomeric state of  $^{172}\text{Ir}$ ; see text for details. (b) Projections on the  $E_\alpha$  axis of the events from the  $^{172}\text{Ir}$  region of (a) by gating on the respective delayed  $\gamma$  rays. Relevant peaks are labeled with their corresponding  $E_\alpha$  values. The intensity scales for the three weaker spectra are adjusted for better visibility.

events unambiguously. The total  $Q_{\alpha,\text{tot}}$  values for these four groups agree well with each other within the experimental uncertainties, i.e.,  $Q_{\alpha,\text{tot}} = 5.768(5)$  MeV for the 89.4 keV  $\gamma$  ray, 5.772(5) MeV for the 102.8 keV  $\gamma$  ray, 5.771(5) MeV for the 123 keV  $\gamma$  ray, and 5.772(5) MeV for the 136 keV  $\gamma$  ray. We therefore conclude that these groups belong to the fine structure of the  $\alpha$  decay from the same state of  $^{172}\text{Ir}$ . This was further confirmed by the half-life for each case, which was obtained by the low-counting horizontal DSSD strips with the strip number larger than 28 or smaller than 6. As given in Fig. 11 and Table I, the half-life values conform with each other within experimental uncertainties and the final weighted average half-life was determined to be 4.1(2) s for the low-spin isomeric state of  $^{172}\text{Ir}$ , which is consistent with previous measurement [34]. However, for the four  $\gamma$ -ray transitions, a clear assignment of multipolarity cannot be determined due to their very close  $\alpha$ -particle energies and the tails of the 5919 keV peak of  $^{171}\text{Ir}$  and the 5818 keV peak of  $^{172}\text{Ir}$ . Since these events in Fig. 9 were observed within short time intervals and no significant correlation with Re  $K_{\alpha,\beta}$  x rays was observed, it is suggested that the multipolarity of these  $\gamma$ -ray transitions is limited to low multipolarity order. In Ref. [34], the strongest 123 keV  $\gamma$  ray was designated as having an  $E1$  multipolarity. For convenience, we tentatively assume that all the other three  $\gamma$ -ray transitions have the  $E1$  multipolarity, and based on this each corresponding branching ratio is roughly obtained and presented in Fig. 11 and Table I, sharing the 2.0(2)% total branching ratio measured in Ref. [34]. The absence of firm multipolarity assignments for the respective  $\gamma$  decays prevents

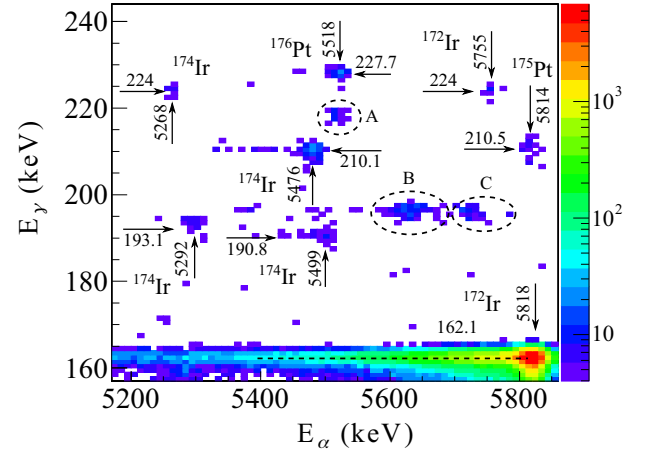


FIG. 10.  $E_\alpha$ - $E_\gamma$  coincidence spectrum with the time interval of  $0 < \Delta t(\gamma-\alpha) < 300$  ns. Each group is annotated with the corresponding energies and the original mother nucleus, of which the  $^{175}\text{Pt}$  and  $^{176}\text{Pt}$  were due to the isotopic impurity in the target. The groups labeled with A, B, and C are due to decays that could not be firmly assigned to any nucleus.

us from drawing any conclusions on the hindrance factors associated with the  $\alpha$ -decay fine structure of  $^{172}\text{Ir}$  as well as on the nature of the excited states in the daughter nucleus  $^{168}\text{Re}$ .

The high-spin isomeric state ( $7^+$ ) of  $^{172}\text{Ir}$  was previously reported to decay to an excited state of  $^{168}\text{Re}$  through an  $E_\alpha = 5.82(1)$  MeV decay followed by a 162.1(1) keV  $\gamma$ -ray transition [33,34]. As mentioned, it was strongly populated in the present measurement. In our work the energy  $E_\alpha = 5.818(4)$  MeV was determined with an associated half-life of 1.89(5) s, which is in good agreement with the previously reported value of 2.0(1) s. [34]. In addition, a new  $\alpha$ -decay branch was observed for the high-spin isomeric-state of  $^{172}\text{Ir}$ , as revealed by the group  $E_\alpha(5755 \text{ keV})$ - $E_\gamma(224 \text{ keV})$  in Fig. 10. The calculated total  $Q_{\alpha,\text{tot}}$  value of 6.116(7) MeV for this branch is within the uncertainty of the value of 6.119(4) MeV for the  $E_\alpha(5818 \text{ keV})$ - $E_\gamma(162.1 \text{ keV})$  branch. Due to its low intensity, the corresponding  $\alpha$ -decay half-life and multipolarity of the 224.0(5) keV  $\gamma$ -ray transition could not be determined. By assuming that the 224.0(5) keV  $\gamma$ -ray transition has an  $M1$  multipolarity and comparing its intensity to the intensity of the 162.1(1) keV  $\gamma$ -ray transition, an upper limit of the branching ratio,  $b_\alpha < 4 \times 10^{-3}$ , for the  $E_\alpha = 5.755(7)$  MeV decay was estimated, as given in Table I and Fig. 11.

### E. $\alpha$ -decay fine structure of $^{174}\text{Ir}$

An  $E_\alpha = 5.275(10)$  MeV decay from the low-spin isomeric state ( $3^+$ ) of  $^{174}\text{Ir}$  was observed by Schmidt-Ott *et al.* to populate a 225 keV excited state of  $^{170}\text{Re}$ , which then deexcites either via a 224.6 keV  $\gamma$ -ray transition or by a cascade of 31.4-193.5 keV  $\gamma$ -ray transitions [34]. They also observed another  $E_\alpha = 5.478$  MeV decay from the high-spin isomeric state ( $7^+$ ) of  $^{174}\text{Ir}$  to a 210.4 keV excited state of  $^{170}\text{Re}$  in coincidence with three  $\gamma$ -ray transitions with energies of 210.3, 190.2, and 20.2 keV, where the 20.2 and 190.2 keV  $\gamma$ -ray transitions constitute a cascade. However, in the present

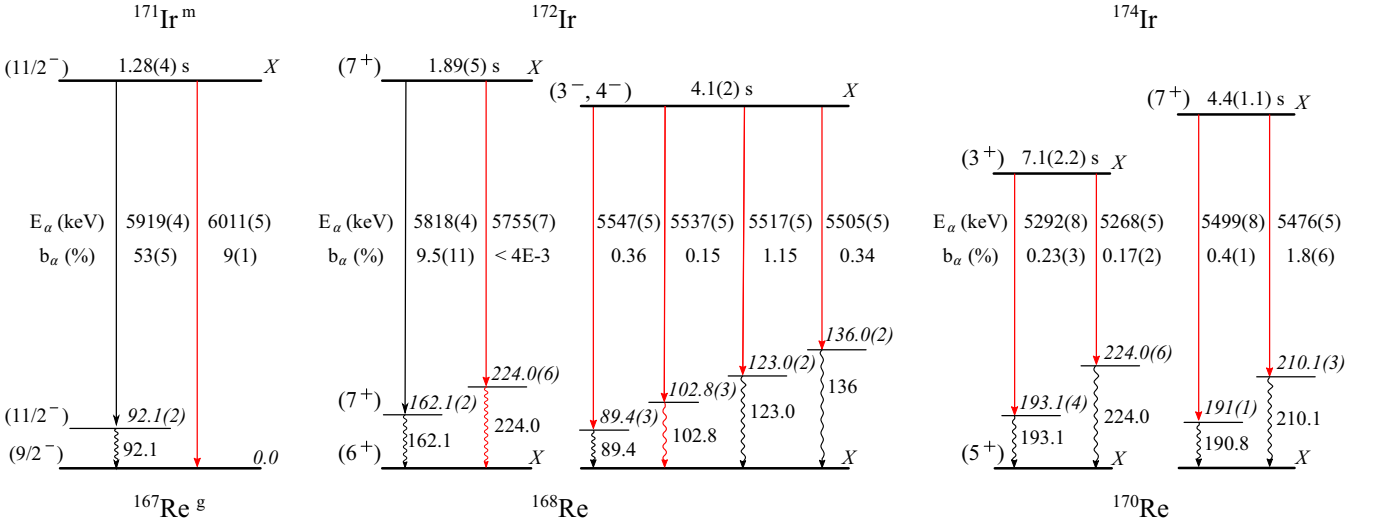


FIG. 11. Decay schemes of  $^{171,172,174}\text{Ir}$  deduced in this work. Some levels are labeled with the symbol  $X$  indicating that their excitation energy relative to the ground state in the corresponding nuclide is unknown. The newly observed transitions are indicated in red. Half-lives determined from this work are shown above the corresponding state. See text and Table I for details.

experiment, we found that each of the 193.5, 224.6, 210.4, and 190.2 keV  $\gamma$ -ray transitions corresponds to its own  $\alpha$  decay, as shown by the four groups associated with  $^{174}\text{Ir}$  in Fig. 10. After checking the total  $Q_{\alpha,\text{tot}}$  values for each  $\alpha$  decay, we propose a new decay scheme for  $^{174}\text{Ir}$ , as shown in Fig. 11, whereby the 5.476(5) and 5.499(8) MeV  $\alpha$  decays feed the respective excited states at 210.1(3) and 191(1) keV of  $^{170}\text{Re}$  from the high-spin isomeric state of  $^{174}\text{Ir}$ , and the  $E_\alpha = 5.292(8)$  and  $E_\alpha = 5.268(5)$  MeV  $\alpha$  decays feed the respective excited states at 193.1(4) and 224.0(6) keV of  $^{170}\text{Re}$  from the low-spin isomeric state of  $^{174}\text{Ir}$ . The previously reported 20.2 and 31.4 keV  $\gamma$ -ray transitions were not observed in this work, presumably due to the low detection efficiency of the GREAT planar HPGe detector at these energies. Referring to the  $\alpha$ -decay branching ratio of each isomeric state measured in Ref. [34], an approximate branching ratio was estimated for each of the four  $\alpha$  decays based on the tentative assumption of  $E1$  multipolarity for the corresponding  $\gamma$ -ray transition, as given in Table I. A half-life of 7.1(2.2) s was determined in this work for the low-spin isomeric state by tagging on the 193.1 or 224.0 keV  $\gamma$  rays, while in a similar way the half-life of the high-spin isomeric state was determined to be 4.4(11) s, both consistent with the previous measurements [34].

#### IV. DISCUSSION

The results obtained from this work have been analyzed within the framework of the universal decay law [35,36], which starts from the microscopic Thomas expression provided by the residues of the  $R$  matrix [37]. The model is designed to consistently describe half-lives related to all forms of cluster radioactivity [35], expressed as

$$T_{1/2} = \frac{\hbar \ln 2}{\Gamma_c} = \frac{\ln 2}{v} \left| \frac{H_l^+(\chi, \rho)}{RF_l(R)} \right|^2, \quad (1)$$

where  $l$  is the angular momentum carried by the emitted cluster with the outgoing velocity  $v$ .  $H_l^+$  is the Coulomb-Hankel

function [38]. The solution to Eq. (1) is found by fixing the radial distance  $R$  at the nuclear surface where the wave function describing the cluster in the mother nucleus is matched with the outgoing cluster-daughter wave function. The penetrability is proportional to  $|H_l^+(\chi, \rho)|^{-2}$  and the quantity  $F_l(R)$  is the  $\alpha$ -cluster formation amplitude. The calculated formation probabilities  $|RF_l(R)|^2$  are shown in Table I together with the reduced  $\alpha$ -decay widths  $\delta^2$  calculated using the Rasmussen approach [39].

With the aim to shed light on the influence of the unpaired valence nucleons on the  $\alpha$ -clustering process, we choose the  $E_\alpha = 5.407$  MeV ground-state  $\alpha$  decay of  $^{170}\text{Os}$  leading to the ground state of  $^{166}\text{W}$  [17] as the reference transition (labeled with the subscript “*ref*” in the following equation) and analyze the hindrance factors (HF) for the decays of  $^{171}\text{Os}$ ,  $^{171}\text{Ir}$ , and  $^{172}\text{Ir}$  as

$$\text{HF} = \left| \frac{F_{\text{ref}}(R)}{F(R)} \right|^2 \approx \frac{\delta_{\text{ref}}^2}{\delta^2}. \quad (2)$$

The hindrance factor is independent of the  $\alpha$ -decay energy and can therefore be used to compare the intrinsic mechanisms that induce the  $\alpha$ -decay process. Both methods give almost identical HF values which are listed in Table I. The  $(5/2^-)$  ground-state  $\alpha$  decay of  $^{171}\text{Os}$  with  $E_\alpha = 5.248$  MeV, the  $(13/2^+)$  state decay of  $^{171}\text{Os}$  with  $E_\alpha = 5.306$  MeV as well as the  $(11/2^-)$  state decay of  $^{171}\text{Ir}$  with  $E_\alpha = 5.919$  MeV, have relatively small HF values. This indicates that for these initial-state configurations the odd valence neutron/proton has little effect on the  $\alpha$ -clustering process, such as a light retardation due to the pairing blocking effect of the odd valence particle as discussed in Ref. [40], where the spin-dependent blocking effect of the neutron  $i_{13/2}$  and  $p_{3/2}$  orbitals is suggested to give rise to a hindrance factor of  $\approx 2-3$  in the  $\alpha$  decays of  $^{193-197}\text{Po}$  relative to the decays in the neighboring even-even Po isotopes. On the other hand, for the odd-odd nucleus  $^{172}\text{Ir}$ , a somewhat larger hindrance factor could then be expected since blocking of pair correlations from both the

valence neutron and proton might come into effect. Taking this into account, the  $E_\alpha = 5818$  keV  $\alpha$  decay of  $^{172}\text{Ir}$ , with an observed hindrance factor of 6.2(9), is therefore considered to be unhindered or only weakly hindered, similarly to the 6080 and 6114 keV  $\alpha$  decays of  $^{176}\text{Au}$  [41].

The low hindrance factors of the 5248, 5168, and 5115 keV  $\alpha$  decays of  $^{171}\text{Os}$  are consistent with that the ground state and the 79.2 and 134.2 keV excited states of  $^{167}\text{W}$  have single-particle configurations similar to the  $(5/2^-)$  parent state, which is assigned to the  $5/2^-$  [523] Nilsson configuration with mixed  $\nu f_{7/2}/h_{9/2}$  parentage [42]. Furthermore, the slowly increasing hindrance factors of these  $\alpha$  decays with decreasing energy is consistent with the trends observed for the  $\alpha$ -decay fine structures of  $^{175}\text{Pt}$  [43] and  $^{177}\text{Pt}$  [17]. This could be an effect resulting from a shape evolution as a function of increasing angular momentum in the daughter nucleus.

The  $E_\alpha = 6011$  keV  $(11/2^-) \rightarrow (9/2^-)$   $\alpha$  decay of  $^{171}\text{Ir}$  is observed to be hindered by a factor of  $\approx 8$  relative to the 5919 keV  $(11/2^-) \rightarrow (11/2^-)$  decay from the same initial state. We note that triaxial shape differences between the final-state signature configurations in  $^{167}\text{Re}$  populated in these  $\alpha$  decays ( $\alpha_s = +1/2$  and  $\alpha_s = -1/2$ , respectively) might increase the relative hindrance on account of differences in the associated  $K$  mixing. Joss *et al.* [44] studied the rotational bands built on these states and noted the differences in the triaxial shape-driving properties between the  $\alpha_s = +1/2$  and  $\alpha_s = -1/2$  signatures of the  $\pi h_{11/2}$  orbital predicted by cranked shell model calculations. They also noted that the larger signature splitting in the  $\pi h_{11/2}$  band structure of  $^{167}\text{Re}$  compared with the heavier rhenium isotopes suggests that the core-polarizing effect of the  $h_{11/2}$  proton drives  $^{167}\text{Re}$  further from axial symmetry at low spin, consistent with the cranked shell model calculations. In this transitional region, triaxiality is a ubiquitous feature observed in several neighboring nuclei, such as  $^{175,176}\text{Pt}$  [45],  $^{169,171,173}\text{Ir}$  [28,46], and  $^{172}\text{Os}$  [47] and attributed to the occupation of core-polarizing valence orbitals from high- $j$  subshells, e.g.,  $h_{9/2}$ ,  $h_{11/2}$ , and  $i_{13/2}$  orbitals which make the nuclear potential soft with respect to triaxial deformation.

The newly observed 4909 keV  $\alpha$  decay of  $^{172}\text{Os}$  has a hindrance factor of 10(4) relative to the ground-state to ground-state 5106 keV  $\alpha$  decay, as shown in Fig. 12(a). This HF value is much higher than the theoretically predicted value of 1.7 by Peltonen *et al.* [48] using the stationary coupled channels approach, although their calculations could reproduce the decay widths to the first  $2^+$  states fairly well in the even-even deformed emitters with  $Z \geq 90$  and  $A \geq 226$ . In their calculation, the collective  $2^+$  state of the daughter nucleus was described within the rigid rotor model and the  $\alpha$ -daughter interaction was given by a double folding procedure (see Ref. [48] for details). The discrepancy observed in the present work suggests the need for further theoretical model development as well as more experimental data on  $\alpha$ -decay fine structure in this shape-transitional region of the nuclear

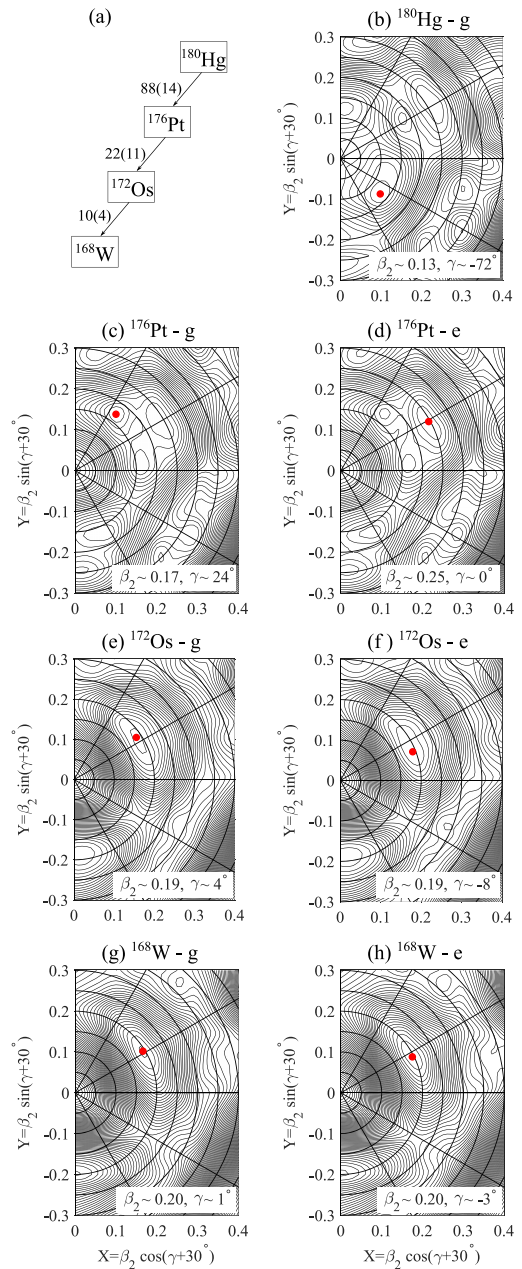


FIG. 12. (a)  $\alpha$ -decay chain from  $^{180}\text{Hg}$  to  $^{168}\text{W}$ . The relative HF value for the fine structure member to the first excited  $2^+$  state of each decay is shown to the left of each arrow, where the data are taken from Ref. [55] and the present measurement on  $^{172}\text{Os}$ . Results of TRS calculations are shown for the ground-state configuration of  $^{180}\text{Hg}$  [labeled (b)] and the ground-state and first excited  $2^+$  states of  $^{176}\text{Pt}$  [(c) and (d), respectively],  $^{172}\text{Os}$  [(e) and (f), respectively], and  $^{168}\text{W}$  [(g) and (h), respectively]. The potential energy surfaces (PES) for the ground  $0^+$  states and the first excited  $2^+$  states were calculated at  $\hbar\omega = 0$  and 0.15 MeV, respectively. The energy difference between contour lines in the PES is 100 keV. Minima in the PES are indicated by red dots with the corresponding deformation parameters shown in each panel. See text for details.

chart. Attempts have been made to calculate the dependence of  $\alpha$ -decay widths on nuclear shape parameters within a microscopic theoretical framework; see, e.g., Refs. [49–51]. Hindrance factors for the  $\alpha$  decays of Rn and Po isotopes were explained to be associated with the potential energy surface calculations, suggesting that moderate changes in deformation might result in a significant change in the hindrance factor [50]. In order to investigate the sensitivity of the observed  $\alpha$ -decay hindrance factors to small shape differences, a systematic analysis of relative hindrance factors for the  $\alpha$ -decay chain of  $^{180}\text{Hg}$  to  $^{168}\text{W}$  was carried out and compared with the results of total Routhian surface (TRS) calculations [52,53]; see Fig. 12. The relative HF values shown in Fig. 12(a) were calculated by comparing the reduced  $\alpha$ -decay widths to the first  $2^+$  states in the daughter nuclei with those of the respective decays to the ground states. In the TRS calculations, we assume  $\hbar\omega = 0$  and 0.15 MeV to be representative for the  $0^+$  ground states and the first excited  $2^+$  state for each nucleus, respectively. The energy minima of the potential energy surfaces (PES) are marked by red dots and the corresponding deformation parameters  $\beta_2$  and  $\gamma$  are labeled in each panel. Overall, a rough correlation between the deduced relative HF and the calculated shape change can be seen for this decay chain. As classic examples of shape coexistence, the ground state of  $^{180}\text{Hg}$  is known to have a weakly deformed oblate shape [54] while the ground state of  $^{176}\text{Pt}$  is known to have a triaxial shape [45], both coexisting with a deformed prolate shape. The large HF value of 88 for the  $\alpha$  decay of  $^{180}\text{Hg}$  to the first  $2^+$  state of  $^{176}\text{Pt}$  [55] can be related to the shape change from a triaxial shape in the ground state to a more prolate deformation in the  $2^+$  state. The HF value of 22 for the  $\alpha$  decay of  $^{176}\text{Pt}$  [55] corresponds to a calculated  $\Delta\gamma \approx 12^\circ$  triaxial shape difference in the daughter nucleus  $^{172}\text{Os}$ , while the HF value of 10 for the  $\alpha$  decay of  $^{172}\text{Os}$  corresponds to a calculated  $\Delta\gamma \approx 4^\circ$  triaxial shape difference in the daughter nucleus  $^{168}\text{W}$ . This suggests that even subtle changes in the nuclear shape parameters, particularly the triaxial degree of freedom, play an important role for  $\alpha$  decay rates. In addition, it is noteworthy that the measured  $2_1^+ \rightarrow 0_{gs}^+$  reduced electric quadrupole transition probabilities,  $B(E2)$ , are 87(8) [56], 115(7) [57], and 117(6) W.u. [58] for the daughter nuclides  $^{176}\text{Pt}$ ,  $^{172}\text{Os}$ , and  $^{168}\text{W}$ , respectively. This supports the evidence that  $\alpha$ -decay fine structure is a sensitive probe of

relatively small changes in the nuclear deformation, providing a valuable complement to measurements of electromagnetic transition rates.

## V. CONCLUSIONS

New and improved data on complex fine-structure  $\alpha$  decays have been established for the neutron-deficient nuclei  $^{171,172}\text{Os}$  and  $^{171,172,174}\text{Ir}$ , providing insights into the low-lying levels in the daughter nuclei. It was found that these  $\alpha$  decays are largely unhindered or weakly hindered, suggesting similar configurations in the corresponding states of the mother and daughter nuclei. Correlations between  $\alpha$ -decay hindrance factors and shape changes are discussed and investigated for the case of the newly observed  $\alpha$ -decay fine structure in  $^{172}\text{Os}$  using total Routhian mean field calculations. The results indicate that small differences in the nuclear shape parameters might significantly affect the  $\alpha$ -decay hindrance factors and hence may serve as a sensitive experimental tool for investigating nuclear deformations. The newly identified  $\alpha$ -decay branch from the bandhead of the  $\nu i_{13/2}$  band in  $^{171}\text{Os}$  is the only one, to date, found in the Os-Pt region, resulting in an unusual competition between  $\alpha$ ,  $\beta$ , and electromagnetic decays from this isomeric state.

## ACKNOWLEDGMENTS

This work was supported by the Swedish Research Council under Grants No. 2019-04880 and No. 2019-04808; the United Kingdom Science and Technology Facilities Council (STFC); the EU 7th Framework Programme, Integrating Activities Transnational Access, Project No. 262010 EN-SAR; and the Academy of Finland under the Finnish Centre of Excellence Programme (Nuclear and Accelerator Based Physics Programme at JYFL). E.I., Y.D.F., and M.K.R. acknowledge support from the International Joint Research Promotion Program of Osaka University. W.Z. acknowledges support from the China Scholarship Council under Grant No. 201700260239. The authors acknowledge the support of the GAMMAPOOL for the JUROGAM detectors. We thank the JYFL Accelerator laboratory staff for excellent operation of the K130 cyclotron and R. Liotta, D. Delion, and R. Wyss for useful discussions.

- 
- [1] K. Heyde and J. L. Wood, *Rev. Mod. Phys.* **83**, 1467 (2011).
  - [2] B. Saygi *et al.*, *Phys. Rev. C* **96**, 021301(R) (2017).
  - [3] T. Grahn *et al.*, *Phys. Rev. C* **94**, 044327 (2016).
  - [4] B. Cederwall *et al.*, *Phys. Rev. Lett.* **121**, 022502 (2018).
  - [5] W. Zhang *et al.*, *Phys. Lett. B* **820**, 136527 (2021).
  - [6] A. Goasduff *et al.*, *Phys. Rev. C* **100**, 034302 (2019).
  - [7] A. N. Andreyev *et al.*, *Nature (London)* **405**, 430 (2000).
  - [8] P. Möller, A. Sierk, T. Ichikawa, and H. Sagawa, *At. Data Nucl. Data Tables* **109-110**, 1 (2016).
  - [9] M. J. Taylor *et al.*, *Nucl. Instrum. Methods Phys. Res., Sect. A* **707**, 143 (2013).
  - [10] C. W. Beausang *et al.*, *Nucl. Instrum. Methods Phys. Res., Sect. A* **313**, 37 (1992).
  - [11] G. Duchêne *et al.*, *Nucl. Instrum. Methods Phys. Res., Sect. A* **432**, 90 (1999).
  - [12] M. Leino *et al.*, *Nucl. Instrum. Methods Phys. Res., Sect. B* **99**, 653 (1995).
  - [13] R. D. Page *et al.*, *Nucl. Instrum. Methods Phys. Res., Sect. B* **204**, 634 (2003).
  - [14] A. N. Andreyev *et al.*, *Nucl. Instrum. Methods Phys. Res., Sect. A* **533**, 422 (2004).
  - [15] I. H. Lazarus *et al.*, *IEEE Trans. Nucl. Sci.* **48**, 567 (2001).
  - [16] P. Rahkila *et al.*, *Nucl. Instrum. Methods Phys. Res., Sect. A* **595**, 637 (2008).
  - [17] <https://www.nndc.bnl.gov/>
  - [18] E. S. Paul *et al.*, *Phys. Rev. C* **51**, 78 (1995).

- [19] A. H. Krulisch and A. C. Axtmann, *Nucl. Instrum. Methods* **55**, 238 (1967).
- [20] J. Manfredi *et al.*, *Nucl. Instrum. Methods Phys. Res., Sect. A* **888**, 177 (2018).
- [21] R. D. Page, P. J. Woods, R. A. Cunningham, T. Davinson, N. J. Davis, A. N. James, K. Livingston, P. J. Sellin, and A. C. Shotton, *Phys. Rev. C* **53**, 660 (1996).
- [22] K. H. Schmidt, C.-C. Sahm, K. Pielenz, and H.-G. Clerc, *Z. Phys. A* **316**, 19 (1984).
- [23] J. Borggreen and E. K. Hyde, *Nucl. Phys. A* **162**, 407 (1971).
- [24] T. Hild, W.-D. Schmidt-Ott, V. Kunze, F. Meissner, C. Wennemann, and H. Grawe, *Phys. Rev. C* **51**, 1736 (1995).
- [25] T. Kibédi, T. W. Burrows, M. B. Trzhaskovskaya, P. M. Davidson, and C. W. Nestor, Jr., *Nucl. Instrum. Methods Phys. Res. Sect. A* **589**, 202 (2008).
- [26] F. P. Hessberger *et al.*, *Nucl. Instrum. Methods Phys. Res., Sect. A* **274**, 522 (1989).
- [27] T.-M. Goon, Alpha and gamma-ray spectroscopic studies of Au, Pt, and Ir nuclei near the proton dripline, Ph.D. thesis, University of Tennessee, Knoxville, 2004, [https://trace.tennessee.edu/utk\\_graddiss/3799](https://trace.tennessee.edu/utk_graddiss/3799).
- [28] R. A. Bark *et al.*, *Nucl. Phys. A* **646**, 399 (1999).
- [29] A. Thornthwaite, Structure of the neutron-deficient nuclei  $^{173}\text{Au}$  and  $^{173}\text{Pt}$  and their  $\alpha$ -decay descendants, Ph.D. thesis, University of Liverpool, 2014, <https://doi.org/10.17638/02005619>.
- [30] M. W. Rowe *et al.*, *Phys. Rev. C* **65**, 054310 (2002).
- [31] A. N. Andreyev *et al.*, *J. Phys. G: Nucl. Part. Phys.* **37**, 035102 (2010).
- [32] U. J. Schrewe, W.-D. Schmidt-Ott, R.-D.v. Dincklage, E. Georg, P. Lemmert, H. Jungclas, and D. Hirdes, *Z. Phys. A* **288**, 189 (1978).
- [33] A. N. Andreyev *et al.*, *Phys. Rev. C* **90**, 044312 (2014).
- [34] W.-D. Schmidt-Ott, H. Salewski, F. Meissner, U. Bosch-Wicke, P. Koschel, V. Kunze, and R. Michaelsen, *Nucl. Phys. A* **545**, 646 (1992).
- [35] C. Qi, F. R. Xu, R. J. Liotta, and R. Wyss, *Phys. Rev. Lett.* **103**, 072501 (2009).
- [36] D. S. Delion, *Theory of Particle and Cluster Emission* (Springer-Verlag, Berlin, 2010).
- [37] R. G. Thomas, *Prog. Theor. Phys.* **12**, 253 (1954).
- [38] R. G. Lovas, R. J. Liotta, A. Insolia, K. Varga, and D. S. Delion, *Phys. Rep.* **294**, 265 (1998).
- [39] J. O. Rasmussen, *Phys. Rev.* **113**, 1593 (1959).
- [40] K. Van de Vel *et al.*, *Phys. Rev. C* **65**, 064301 (2002).
- [41] R. D. Harding *et al.*, *Phys. Rev. C* **104**, 024326 (2021).
- [42] K. Theine *et al.*, *Nucl. Phys. A* **548**, 71 (1992).
- [43] P. Peura *et al.*, *Phys. Rev. C* **89**, 024316 (2014).
- [44] D. T. Joss *et al.*, *Phys. Rev. C* **68**, 014303 (2003).
- [45] B. Cederwall *et al.*, *Z. Phys. A* **337**, 283 (1990).
- [46] M. Sandzelius *et al.*, *Phys. Rev. C* **75**, 054321 (2007).
- [47] J. C. Wells, N. R. Johnson, C. Baktash, I. Y. Lee, F. K. McGowan, M. A. Riley, A. Virtanen, and J. Dudek, *Phys. Rev. C* **40**, 725 (1989).
- [48] S. Peltonen, D. S. Delion, and J. Suhonen, *Phys. Rev. C* **78**, 034608 (2008).
- [49] D. S. Delion, A. Florescu, M. Huyse, J. Wauters, P. Van Duppen, A. Insolia, and R. J. Liotta, *Phys. Rev. C* **54**, 1169 (1996).
- [50] D. Karlgren, R. J. Liotta, R. Wyss, M. Huyse, K. Van de Vel, and P. Van Duppen, *Phys. Rev. C* **73**, 064304 (2006).
- [51] D. E. Ward, B. G. Carlsson, and S. Åberg, *Phys. Rev. C* **92**, 014314 (2015).
- [52] R. Wyss, J. Nyberg, A. Johnson, R. Bengtsson, and W. Nazarewicz, *Phys. Lett. B* **215**, 211 (1988).
- [53] W. Nazarewicz, R. Wyss, and A. Johnson, *Nucl. Phys. A* **503**, 285 (1989).
- [54] T. Grahm *et al.*, *Phys. Rev. C* **80**, 014324 (2009).
- [55] B. Pritychenko *et al.*, *Nucl. Instrum. Methods Phys. Res., Sect. A* **640**, 213 (2011).
- [56] G. D. Dracoulis, A. E. Stuchbery, A. P. Byrne, A. R. Poletti, S. J. Polett, J. Gerl, and R. A. Bark, *J. Phys. G: Nucl. Phys.* **12**, L97 (1986).
- [57] A. Virtanen, N. R. Johnson, F. K. McGowan, I. Y. Lee, C. Baktash, M. A. Riley, J. C. Wells, and J. Dudek, *Nucl. Phys. A* **591**, 145 (1995).
- [58] G. D. Dracoulis, G. D. Sprouse, O. C. Kistner, and M. H. Rafailovich, *Phys. Rev. C* **29**, 1576 (1984).